Lithium-Ion Batteries

DOI: 10.1002/anie.201003743

Scalable Synthesis of Tavorite $LiFeSO_4F$ and $NaFeSO_4F$ Cathode Materials**

*Rajesh Tripathi, T. N. Ramesh, Brian L. Ellis, and Linda F. Nazar**

Rechargeable lithium-ion cells are considered the most advanced energy storage systems. Commercial cells utilize layered metal-based oxides as the positive electrode,[1] but their high cost and safety could limit use in large-scale applications. In an intensive search for alternative materials, phosphates such as $LiFePO_4$,[2–5] and other polyanion ("XO_4") structures have also been explored, including those based on silicates.[6] In addition to possessing high redox potentials and promising Li^+ transport, polyanion frameworks can exhibit remarkable electrochemical and thermal stability. These make them particularly suitable where safety and longevity are a concern. Fluorinated polyanion moieties have also received much attention owing to their similar properties. The addition of fluoride engenders a charge difference and modification to the dimensionality of the lattice along with an increase in redox potential, thus offering the tantalizing promise of new architectures and electrochemical behavior.[7] 2D layered alkali iron fluorophosphates A_2FePO_4F (A = Na, Li) have been reported[8]—as well as a family of 3D alkali metal fluorophosphate ion conductors known as tavorites. Named after the mineral $LiFePO_4OH$,[9] this structure does not display the inherent limitations of the 1D ion conductivity of the well-known $LiFePO_4$ olivine lattice. The tavorite framework possesses intersecting channels housing Li^+ that afford multidimensional pathways for ion transport. It is adopted by many minerals;[10] and the redox-active $LiMPO_4F$ members (V, Fe, Ti, Mn) exhibit excellent electrochemical properties.[11–13] The newest member of the tavorite family, $LiFeSO_4F$, is reported to be an exciting intercalation host that is anticipated to vie with the stellar $LiFePO_4$ for prominence on the basis of its superior electrochemical properties.[14] These can be achieved with submicron—not nanosized—particles providing considerable advantages for material processing, and the opportunity for even faster rate behavior with further decrease in ion transport path length.

The synthesis of $LiFeSO_4F$ cannot be accomplished by typical solid-state routes, however. This is due to its low thermodynamic stability in comparison to the temperatures needed to overcome the kinetics necessary for reaction to occur. It was reported that its poor hydrolytic stability, and that of other related $LiMFSO_4$ fluorosulfates means that crystallization must be effected at low (< 400 °C) temperatures in hydrophobic ionic liquids (ILs) in order to control the reactivity of the hydrated iron precursor.[14,15] IL media have been demonstrated to be an elegant and versatile means to facilitate reactivity at intermediate temperatures.[16] Nonetheless, such exotic solvents, while offering much promise of tailoring reactivity, are prohibitively expensive at ca. $500/g, and removal of excess LiF reagent is almost impossible owing to its low solubility. Here we demonstrate that single-phase tavorite $LiFeSO_4F$ is easily crystallized by reaction in hydrophilic tetraethylene glycol at 220 °C to give a highly electrochemically active material. The use of the low-cost solvent obviates the necessity of recycling precious ionic liquids. Reversible Li insertion is facilitated by the close structural similarity of the lattice with the parent tavorite-type monoclinic $C2_1/c$ $FeSO_4F$ framework, whose structure we have solved. We furthermore show that a new possible Na-ion battery material, $NaFeSO_4F$, can be similarly synthesized as a single phase that is closely related to tavorite. Control of reaction parameters leads to ca. 200 nm homogeneously sized crystallites which exhibit surprising ion mobility properties. Our synthetic approach relies on the formation of macroporous $FeSO_4{\cdot}H_2O$ formed by rapidly heating $FeSO_4{\cdot}7H_2O$ in a N_2/7 % H_2 atmosphere, and reacting this with either NaF or LiF in tetraethylene glycol (TEG) at 220 °C for 60 h (Li) or 48 h (Na). The materials were shown to be single phase as determined by X-ray diffraction (XRD) and field emission scanning electron microscopy (FESEM).

The structure type of $MSO_4{\cdot}H_2O$ has a strong topological resemblance to the tavorite structure of the fluorosulfate $LiMSO_4F$, as noted.[17–19] The H–OH in $MSO_4{\cdot}H_2O$ (or $HMSO_4OH$) is replaced by Li–F to generate $LiMSO_4F$. As previously described, the reaction between the alkali metal fluorides and $FeSO_4{\cdot}H_2O$ involves two simultaneous processes: 1) loss of water from $FeSO_4{\cdot}H_2O$ and 2) insertion of LiF or NaF in the structure. To obtain a pure product, the reaction rate (step 2) must be higher than the dehydration rate (step 1) to avoid the crystallization of $FeSO_4$. In previous studies it was argued that a hydrophobic reaction medium is crucial to slow down the dehydration, so that the reaction with LiF can proceed. However, the opposite approach is more effective: namely, the reaction can be performed in a hydrophilic organic solvent such as TEG (Scheme 1). The reaction proceeds by the dissolution of LiF (or NaF) in the solvent (which is sparingly soluble in TEG at elevated temperature) followed by exchange with the H_2O molecule in $FeSO_4{\cdot}H_2O$. The reaction must be performed at temperatures low enough to minimize the dehydration of the iron sulfate precursor to

[*] R. Tripathi, T. N. Ramesh, B. L. Ellis, Prof. L. F. Nazar
Department of Chemistry, University of Waterloo
200 University Avenue West, Waterloo Ontario N2L 3G1 (Canada)
Fax: (+1) 519-746-0435
E-mail: lfnazar@uwaterloo.ca

[**] This work was carried out with the financial support of the Canadian Natural Sciences and Engineering Council through their Discovery and Canada Research Chair programs.

Supporting information for this article is available on the WWW under http://dx.doi.org/10.1002/anie.201003743.

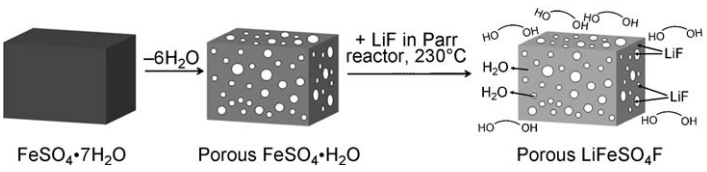

Scheme 1. Diagram illustrating the methodology for solvothermal synthesis of $LiFeSO_4F$ and $NaFeSO_4F$.

unreactive $FeSO_4$. Temperatures as low as 220 °C are ideal, as $FeSO_4{\cdot}H_2O$ dehydrates in air at temperatures > 230 °C. Our synthetic method incorporates three important factors which increase reaction rate and facilitate conversion of reagents to products. First, optimized rapid heating of the $FeSO_4{\cdot}7H_2O$ to produce $FeSO_4{\cdot}H_2O$ results in a spongy macroporous morphology which is faithfully replicated in the topotactic reaction to yield $LiFeSO_4F$ (see the Supporting Information 1x). This is critical to facilitate solvent ingress and reactivity. The porous material initially crystallized can be collapsed to fully dense tavorite by heat treatment at 200 °C under N_2. Both materials exhibit the same XRD pattern. The morphology has profound ramifications for the electrochemical performance. Second, milling of the reactants ensures a smaller particle size of the $FeSO_4{\cdot}H_2O$ precursor and intimate mixing with LiF. Last, the hydrophilic medium partially dissolves the LiF or NaF, thereby facilitating access and reactivity. Thus these factors speed up the reaction—as opposed to slowing down the dehydration—thus favoring the topotactic conversion at lower temperatures and reducing the energy and materials cost of producing $LiFeSO_4F$. The structure and phase purity of triclinic $LiFeSO_4F$ (Figure 1 a) was confirmed by Rietveld refinement of the XRD pattern in the space group $P\bar{1}$ using the GSAS platform[20] with EXPGUI interface;[21] very good agreement factors were obtained. The lattice constants and structure are similar to those recently reported,[14] although we obtain more typical Li–O bond lengths (SI 2x, 3x). The structure of $LiFeSO_4F$ corresponds to that of previously described tavorite materials of the same space group.[9] In addition to the low-cost efficiency, another advantage of our synthetic methodology is the purity of the $LiFeSO_4F$ which can be produced. The very low solubility of LiF in hydrophobic ionic liquid media means that its contamination in the product is almost inevitable. The reaction in TEG, conversely, results in almost phase-pure $LiFeSO_4F$ with only a trace of LiF evident (2% from Rietveld refinement). FESEM and energy dispersive spectroscopy (EDS) measurements were also used to examine the morphological aspects and phase purity of the crystallites. The FESEM image (SI Figure 1 a, inset) indicates the crystallites are comprised of irregularly shaped but facetted submicron particles between 400 and 900 nm in dimension. Quantification from EDS spectra recorded on numerous particles revealed the Fe:S:F molar ratio to be close to 1:1:1 in accord with the chemical formula of the fluorosulfate. In thermogravimetric analysis, less than 1% weight loss occurs up to 400 °C in an N_2 atmosphere (SI 4x).

The high theoretical specific capacity of $LiFeSO_4F$ (151 $mAh\,g^{-1}$) has led to its proposal and realization as a suitable new cathode material. The electrochemical behavior of the TEG-synthesized $LiFeSO_4F$ is shown in Figure 2. At a C/10 rate, a reversible capacity of 0.86 Li (130 $mAh\,g^{-1}$) was sustained on cycling at an average potential of 3.6 V (Figure 2 a), with no capacity fading on cycling (not shown). Two-thirds of the theoretical capacity (100 $mAh\,g^{-1}$) is accessible at a rate of C/2.

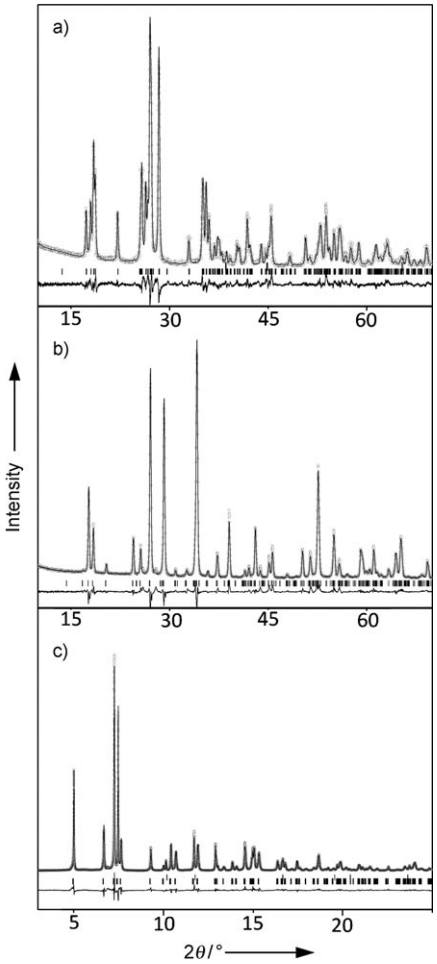

Figure 1. X-ray powder diffraction pattern with the experimental data (gray dots), calculated pattern (black line), Bragg positions (markers), and difference curve shown for a) $LiFeSO_4F$ (λ_{Cu}): $P\bar{1}$, $a = 5.1751(1)$ Å, $b = 5.4915(1)$ Å, $c = 7.2211(2)$ Å, $\alpha = 106.506(2)°$, $\beta = 107.178(2)°$, $\gamma = 97.865(2)°$, $V = 182.441(5)$ Å^3; b) $NaFeSO_4F$ (λ_{Cu}): $P2_1/c$, $a = 6.6739(1)$ Å, $b = 8.6989(2)$ Å, $c = 7.1869(2)$ Å, $\beta = 113.525(2)°$, $V = 382.567(9)$ Å^3. c) $FeSO_4F$ ($\lambda_{0.4122Å}$): $C2/c$, $a = 7.3037(1)$; $b = 7.0753(1)$; $c = 7.3117(1)$, $\beta = 119.758(2)°$, $V = 328.017(8)$ Å^3.

Increasing the cycling rate from C/10 to C/2 increases the polarization only slightly, indicating that the kinetics are rapid in this material owing to its excellent structural characteristics. The electrochemical properties are similar to those reported for material prepared from ILs. The key does not lie only in the solvent, but in the particle morphology. Heat treatment at 200 °C results in partial collapse of the porous structure to form dense crystallites of the same size, but with inferior electrochemical performance (SI 1x). Thus the slightly spongy nature of the electrode material is perfectly

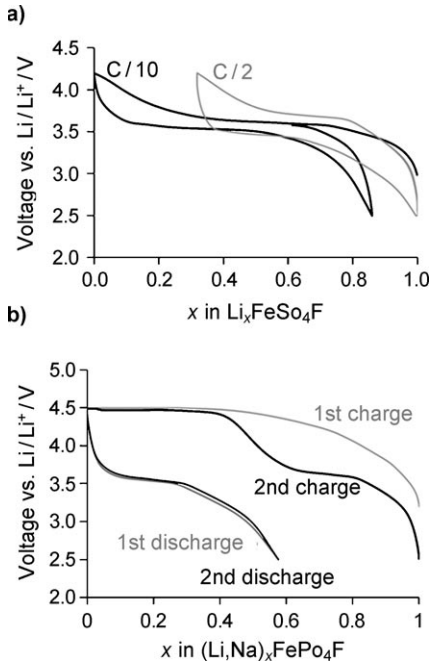

Figure 2. Electrochemical charge–discharge profiles for a) $LiFeSO_4F$; b) $NaFeSO_4F$ at C/10. The first and second discharge curves for $NaFeSO_4F$ are shifted to eliminate the electrolyte oxidation component on charge.

optimized for electrolyte ingress and good kinetics. The rapid 3D ion transport characteristics of the framework at the atomic level, and comparable energy density to that of $LiFePO_4$ owing to its higher voltage (543 $Wh\,kg^{-1}$ vs. 581 $Wh\,kg^{-1}$) also auger well for its future importance as a practical electrode material.

$LiFeSO_4F$ can be readily oxidized with $NOBF_4$ in acetonitrile to produce the empty host framework, $FeSO_4F$. Its XRD pattern is the same as that derived through electrochemical oxidation, but is free of any contaminants arising from the cell. To obtain unequivocal structural information on this phase in order to better understand the electrochemical redox process, a diffraction pattern was collected using a synchrotron source which affords higher intensity and resolution. The diffraction pattern shown in Figure 1c was indexed, and the structure readily refined in a monoclinic cell (space group $C2/c$, no. 15). Details of the fitting procedure can be found in the Supporting Information (5x). This cell is doubled with respect to the triclinic $P\bar{1}$ cell of $LiFeSO_4F$, and differs from the $FeSO_4F$ structure that was proposed, but not resolved.[14] Notable is that the equivalent unit cell volumes of the parent $LiFeSO_4F$ (182.4 $Å^3$), and delithiated ($FeSO_4F$: 164.0 $Å^3$) phases differ by 10.1 %. This is far greater than the volume contraction reported for the olivine $LiFePO_4 \leftrightarrow FePO_4$ of 6.7 %.[2] Coupled with the change in cell symmetry, it suggests that considerable strain should be associated with the redox-driven phase transition. However, the very favorable electrochemical properties (even in the absence of a surface carbon coating) prove otherwise. We speculate that highly effective ion mobility in the tavorite lattice along with limited solid solution behavior overide the other factors, including poor electronic conductivity.

The novel Na-insertion compound, $NaFeSO_4F$, can also be synthesized using the same approach. We,[8] and others,[22] have particular interest in the viability of Na-ion electrode materials, owing to the high natural abundance of Na compared to Li. We prepared $NaFeSO_4F$ using the same methodology as for $LiFeSO_4F$, although the reaction time required is shorter (48 h) owing to the higher solubility of NaF in TEG compared to LiF. The FESEM image (SI 6x) reveals that the crystallites comprise homogenously sized, spherical submicron particles centered at 200 nm in dimension. Quantification from EDS spectra revealed the Na/Fe/S/F molar ratio to be close to 1:1:1:1. The structure of $NaFeSO_4F$ was determined by Rietveld refinement of the XRD pattern (Figure 1b, SI 7x) in a monoclinic cell (space group $P2_1/c$, no. 14). The structural features are compared with those of $LiFeSO_4F$ in Figure 3. The architectural motifs of the two metal fluorosulfate frameworks are very similar, but not identical, as will be discussed below. This leads to profound ramifications in the electrochemical behavior.

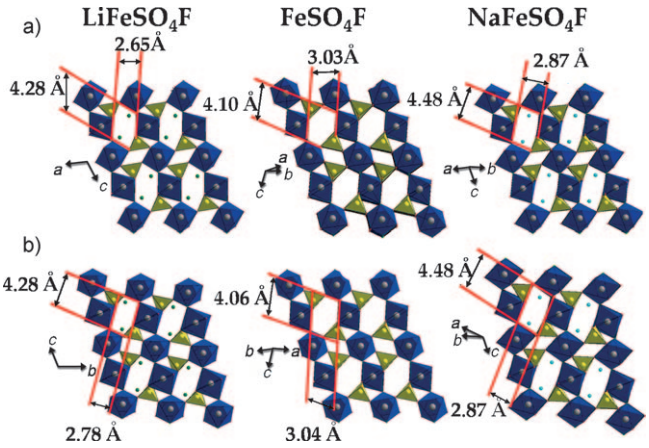

Figure 3. Structures of $LiFeSO_4F$, $FeSO_4F$, and $NaFeSO_4F$ along the equivalent crystallographic directions indicated. The upper structure set (a) and lower set (b) are views along the two tunnels that are almost perpendicular to each other.

The results of electrochemical cycling of $NaFeSO_4F$ in a Li-electrolyte cell cycled between 2.5 V and 4.5 V vs. Li/Li^+ at a rate of C/20 are shown in Figure 2b. On the initial charge cycle, a large overpotential is sustained up to 4.5 V, and there is no indication of a two-phase region indicative of Na extraction. Nonetheless, upon discharge, a plateau near 3.55 V is observed (as in $LiFeSO_4F$) and 55 % of the theoretical capacity is achieved. We conclude that half the Na^+ is removed from the $NaFeSO_4F$ lattice on charge, possibly by ion-exchange with Li^+ in the electrolyte as the first step. The fraction of $FeSO_4F$ generated on charge becomes active for subsequent reversible Li^+ insertion, and the second charge cycle is different from the first. The re-inserted Li^+ is extracted near 3.65 V, and the same capacity is obtained as on first discharge. Additional overcharge to 4.5 V on the second charge does not increase the capacity of the subsequent discharge step (Figure 2b), indicating that some portion of the material is poorly accessible. Na^+ could be

completely extracted from $NaFeSO_4F$ using an oxidizing agent, but more forcing conditions (1M $NOBF_4$ in acetonitrile for 4 d) were required compared to $LiFeSO_4F$. The XRD pattern of the resultant $FeSO_4F$ showed peak broadening that is indicative of crystallite strain (SI 8x).

The difference in behavior between the two $AFeSO_4F$ materials is rooted in their structures. Common to both tavorite-type structures are the linear chains of corner-sharing FeO_4F_2 octahedra which propagate along the *c* axis. These are bridged by corner-sharing SO_4 tetrahedra along the *a* and *b* axes to create a cavernous 3D network, and two large intersecting tunnels for ion migration. Views down these tunnels are compared in Figure 3 for equivalent directions that take into account the difference in cell symmetry. What is most striking is the structural similarity within the family. Differences in the relative rotation and disposition of the framework polyhedra give rise to slightly nonequivalent pathways for ion migration. The tunnels shown are at 85° for $LiFeSO_4F/FeSO_4F$ and at 75° for $NaFeSO_4F$. The larger tunnel size for $NaFeSO_4F$ reflects the larger size of the Na^+ vs. the Li^+ ion. De-alkylation of the lattice results in a small "twist" to give a wider tunnel in both cases. This clearly explains the facile redox behavior of the Li analogue. The question is why the Na analogue has a higher activation energy for ion mobility.

Consideration of the framework provides several clues. In the case of $LiFeSO_4F$, the Li ions reside in large six-coordinate sites within the channels, with the position being split between two sites about 0.8 Å apart (based on single-crystal XRD studies on isostructural $LiAlPO_4F$[23]), equivalent to a very large atomic displacement parameter. This is suggestive of a high degree of ion mobility, in accord with conductivity measurements; neutron diffraction experiments are underway to elucidate the site occupancy. In $NaFeSO_4F$, however, the Na^+ ion is fixed in a single tight six-coordinate site. Comparison of the bond sums for Li^+–O(F) in $LiFeSO_4F$ (0.99) and Na^+–O(F) in $NaFeSO_4F$ (1.16) indicate that the alkali metal ion is much more tightly held in $NaFeSO_4F$. Last of all, the large volume difference between $NaFeSO_4F$ (382.6 $Å^3$)↔$FeSO_4F$ of 14.3%, compared to that of the Li analogue (10.1%) creates additional strain during redox activity and impedes mobility of the two-phase boundary.

In conclusion, we have demonstrated a scalable synthesis route to single-phase $LiFeSO_4F$ that is broadly applicable to a range of related materials. Excellent electrochemical properties are exhibited. We anticipate these can be further improved by tailoring the glycol media to further decrease particle size. Because of the ease of solvothermal synthesis to form a variety of metastable alkali metal polyanion frameworks with new architectures in a simple and cost-effective manner, the method described in this study will significantly broaden our ability to explore these as cathode materials. We furthermore show that ion mobility in the closely related $NaFeSO_4F$ tavorite framework is strongly governed by subtle factors that relate to the depth of the "thermodynamic well" of the mobile ion, and lattice strain on ion extraction. These topics will be further elucidated by our upcoming theoretical and electrochemical studies on these intriguing materials.

Experimental Section

$FeSO_4{\cdot}H_2O$ was prepared by rapidly heating $FeSO_4{\cdot}7H_2O$ for 3 h at 100 °C under a N_2/7% H_2 atmosphere, and ball-milling it with either NaF or LiF (Alfa Aesar > 99.9%) in a 1:1.1 ratio for 24 h in acetone. The mixture was transferred into a 43 mL Teflon-lined Parr reactor along with 30 mL of tetraethylene glycol (TEG) and was stirred for 30 min prior to being heated at 220 °C for 60 h (Li) or 48 h (Na). The resulting gray powders were washed with acetone and collected by centrifugation.

X-ray diffraction (XRD) was carried out on a Bruker D8-Advance operating with $Cu_{K\alpha}$ radiation or on beamline 11-BM at the Advanced Photon Source (APS) at the Argonne National Laboratory using an average wavelength of 0.4122 Å. FESEM imaging was performed on a LEO 1530 field-emission SEM.

Electrochemical measurements were carried out by casting electrodes composed of active material/carbon black/polyvinylidene fluoride binder in a 75:15:10 ratio. The carbon and active material were ball-milled for 1 h at 300 rpm and slurry-cast onto Al foil, with an average loading of 5 $mg\,cm^{-2}$. Electrodes were assembled in 2020 coin cells, using EC/DMC/$LiPF_6$ as the electrolyte.

Received: June 18, 2010
Revised: August 8, 2010
Published online: October 12, 2010

Keywords: lithium fluorosulfate · lithium-ion battery · sodium-ion battery · solvothermal synthesis

[1] M. M. Thackeray, J. O. Thomas, M. S. Whittingham, *MRS Bull.* **2000**, *25*, 39.
[2] A. K. Padhi, K. S. Nanjndaswamy, J. B. Goodenough, *J. Electrochem. Soc.* **1997**, *144*, 1188.
[3] A. S. Andersson, J. O. Thomas, B. Kalska, L. Häggström, *Electrochem. Solid-State Lett.* **2000**, *3*, 66.
[4] A. Yamada, K. Hinokuma, *J. Electrochem. Soc.* **2001**, *148*, A224.
[5] H. Huang, S.-C. Yin, L. F. Nazar, *Electrochem. Solid-State Lett.* **2001**, *4*, A170.
[6] a) S. Nishimura, R. Hayase, M. Kanno, Y. N. Nakayama, A. Yamada, *J. Am. Chem. Soc.* **2008**, *130*, 13212–13213; b) A. Nyten, A. Abouimrane, M. Armand, T. Gustafsson, J. O. Thomas, *Electrochem. Commun.* **2005**, *7*, 156–160.
[7] a) S.-C. Yin, P. Subramanya Herle, A. Higgins, N. J. Taylor, Y. Makimura, L. F. Nazar, *Chem. Mater.* **2006**, *18*, 1745; b) B. Ellis, D. H. Ryan, L. F. Nazar, *Chem. Mater.* **2010**, *22*, 1059.
[8] B. Ellis, W. R. M. Makahnouk, Y. Makimura, K. Toghill, L. F. Nazar, *Nat. Mater.* **2007**, *6*, 749.
[9] W. H. Baur, *Beitr. Mineral. Petrogr.* **1959**, *6*, 399.
[10] a) A. C. Roberts, P. J. Dunn, J. D. Grice, D. E. Newbury, E. Dale, W. L. Roberts, *Powder Diffr.* **1988**, *3*, 93; b) V. I. Simonov, N. V. Belov, *Kristallografiya* **1958**, *3*, 429; c) L. A. Groat, M. Raudsepp, F. C. Hawthorne, T. S. Ercit, B. Sherriff, J. S. Hartmann, *Am. Mineral.* **1990**, *75*, 992.
[11] a) J. Barker, M. Y. Saidi, J. Swoyer, *J. Electrochem. Soc.* **2004**, *151*, A1670; b) J. Barker, M. Y. Saidi, J. Swoyer, U.S. Pat. 0163669, **2005**.
[12] N. Recham, J.-N. Chotard, J.-C. Jumas, L. Laffont, M. Armand, J.-M. Tarascon, *Chem. Mater.* **2010**, *22*, 1142–1148.
[13] T. N. Ramesh, K. T. Lee, L. F. Nazar, *Electrochem. Solid-State Lett.* **2010**, *13*, A47.
[14] N. Recham, J.-N. Chotard, L. Dupont, C. Delacourt, W. Walker, M. Armand, J.-M. Tarascon, *Nat. Mater.* **2010**, *9*, 68.
[15] P. Barpanda, N. Recham, J.-N. Chotard, K. Djellab, W. Walker, M. Armand, J.-M. Tarascon, *J. Mater. Chem.* **2010**, *20*, 1659–1668.

[16] J.-M. Tarascon, N. Recham, M. Armand, J.-N. Chotard, P. Barpanda, W. Walker, L. Dupont, *Chem. Mater.* **2010**, *22*, 724–739.
[17] L. Sebastian, J. Gopalkrishnan, Y. Piffard, *J. Mater. Chem.* **2002**, *12*, 374.
[18] N. Marx, L. Croguennec, D. Carlier, L. Bourgeois, P. Kubiak, F. Le Cras, C. Delmas, *Chem. Mater.* **2010**, *22*, 1099.
[19] M. Anji Reddy, V. Pralong, V. Caignaert, U. V. Varadaraju, B. Raveau, *Electrochem. Commun.* **2009**, *11*, 1807.
[20] A. C. larson, R. B. von Dreele, *Los Alamos National Laboratory Report LAUR* **2000**, 86-*748*.
[21] B. H. Toby, *J. Appl. Crystallogr.* **2001**, *34*, 210.
[22] N. Recham, J. N. Chotard, L. Dupont, K. Djellab, M. Armand, J.-M. Tarascon, *J. Electrochem. Soc.* **2009**, *156*, A993.
[23] L. A. Groat, B. C. Chakoumakos, D. H. Brouwer, C. M. Hoffman, C. A. Fyfe, H. Morell, A. J. Schultz, *Am. Mineral.* **2003**, *88*, 195.

